The Journal of Immunology

ORMDL3 Transgenic Mice Have Increased Airway Remodeling and Airway Responsiveness Characteristic of Asthma

Marina Miller, Peter Rosenthal, Andrew Beppu, James L. Mueller, Hal M. Hoffman, Arvin B. Tam, Taylor A. Doherty, Matthew D. McGeough, Carla A. Pena, Maho Suzukawa, Maho Niwa and David H. Broide

J Immunol 2014; 192:3475-3487; Prepublished online 12 March 2014;
doi: 10.4049/jimmunol.1303047
http://www.jimmunol.org/content/192/8/3475

The Journal of Immunology is published twice each month by
The American Association of Immunologists, Inc.,
9650 Rockville Pike, Bethesda, MD 20814-3994.

Print ISSN: 0022-1767 Online ISSN: 1550-6606.

ORMDL3 Transgenic Mice Have Increased Airway Remodeling and Airway Responsiveness Characteristic of Asthma

Marina Miller,* Peter Rosenthal,* Andrew Beppu,* James L. Mueller,*,† Hal M. Hoffman,*,† Arvin B. Tam,‡ Taylor A. Doherty,* Matthew D. McGeough,*,† Carla A. Pena,*,† Maho Suzukawa,* Maho Niwa,‡ and David H. Broide*

Orosomucoid-like (ORMDL)3 has been strongly linked with asthma in genetic association studies. Because allergen challenge induces lung ORMDL3 expression in wild-type mice, we have generated human ORMDL3 zona pellucida 3 Cre (hORMDL3$^{zp3\text{-}Cre}$) mice that overexpress human ORMDL3 universally to investigate the role of ORMDL3 in regulating airway inflammation and remodeling. These hORMDL3$^{zp3\text{-}Cre}$ mice have significantly increased levels of airway remodeling, including increased airway smooth muscle, subepithelial fibrosis, and mucus. hORMDL3$^{zp3\text{-}Cre}$ mice had spontaneously increased airway responsiveness to methacholine compared to wild-type mice. This increased airway remodeling was associated with selective activation of the unfolded protein response pathway transcription factor ATF6 (but not Ire1 or PERK). The ATF6 target gene SERCA2b, implicated in airway remodeling in asthma, was strongly induced in the lungs of hORMDL3$^{zp3\text{-}Cre}$ mice. Additionally, increased levels of expression of genes associated with airway remodeling (TGF-β1, ADAM8) were detected in airway epithelium of these mice. Increased levels of airway remodeling preceded increased levels of airway inflammation in hORMDL3$^{zp3\text{-}Cre}$ mice. hORMDL3$^{zp3\text{-}Cre}$ mice had increased levels of IgE, with no change in levels of IgG, IgM, and IgA. These studies provide evidence that ORMDL3 plays an important role in vivo in airway remodeling potentially through ATF6 target genes such as SERCA2b and/or through ATF6-independent genes (TGF-β1, ADAM8). *The Journal of Immunology*, **2014, 192: 3475–3487.**

Orosomucoid-like (ORMDL)3 is a gene localized to chromosome 17q21, which was initially linked to asthma in a genome-wide association study (1) with subsequent confirmation in multiple additional genome-wide association studies (2–4) and non– genome-wide association study genetic association studies in populations of diverse ethnic backgrounds (5–10). ORMDL3 has been linked to severe asthma (4, 9), childhood onset of asthma (1, 7, 8), exposure of children to environmental tobacco smoke, and risk of asthma (2, 10), as well as to rhinoviral wheezing illness and genetic risk of childhood onset of asthma (11), underscoring the importance of understanding its function. ORMDL3 is a member of the three member ORMDL gene family (ORMDL1, -2, -3), which encodes transmembrane proteins located at the endoplasmic reticulum (ER) (12). ORMDL1 (chromosome 2) (12) and ORMDL2 (chromosome 12) (12) are on different chromosomes from ORMDL3 (chromosome 17q21) (12) and have not been linked to asthma. Both humans and mice express the same three ORMDL family members, with ORMDL3 exhibiting 96% identity between these two species (12). ORMDL3 is a 153-aa protein with two predicted transmembrane domains (12). We recently demonstrated that in wild-type (WT) mice, ORMDL3 is an allergen and Th2 cytokine (IL-4 or IL-13) inducible gene localized to the ER and highly expressed in airway epithelial cells (13). Allergen challenge induced a 127-fold increase in ORMDL3 mRNA in bronchial epithelium in WT mice, with lesser 15-fold increases in ORMDL2 and no changes in ORMDL1 (13). We also demonstrated that transfection of ORMDL3 in human bronchial epithelial cells in vitro induced expression of CC chemokines (CCL20, also known as MIP-3α) (13), CXC chemokines (IL-8; CXCL10, also known as IFN-γ–induced protein 10 [IP-10]; CXCL11, also known as IFN-inducible T cell α [ITAC]) (13), metalloproteases (matrix metalloproteinase [MMP]-9; a disintegrin and metalloproteinase domain–containing protein 8 [ADAM8]) (13), and selectively activated activating transcription factor 6 (ATF6) (13), one of three ER unfolded protein response (UPR) pathway transcription factors (14) with subsequent regulation of sarco/endoplasmic reticulum Ca^{2+} ATPase (SERCA2b), which has been implicated in airway remodeling in asthma (15). Thus, these studies with bronchial epithelium in WT mice and in normal human bronchial epithelial cells suggest an important role for a pathway in which initial induction of ORMDL3 with subsequent activation of both ATF6-dependent pathways (i.e., SERCA2b) and/or ATF6-independent pathways

*Department of Medicine, University of California, San Diego, La Jolla, CA 92093; †Department of Pediatrics, University of California, San Diego, La Jolla, CA 92093; and ‡Department of Biology, University of California, San Diego, La Jolla, CA 92093

Received for publication November 12, 2013. Accepted for publication February 4, 2014.

This work was supported by National Institutes of Health Grants AI 107779, AI 38425, AI 70535, and AI 72115 (to D.H.B.); National Institutes of Health Grant GM087415 and American Cancer Society Grant RSG10-027-01 (to M.N.); and by National Institutes of Health Grant K08 AI080938 and the American Academy of Allergy, Asthma, and Immunology/American Lung Association (to T.D.).

Address correspondence and reprint requests to Dr. David Broide, Department of Medicine, University of California, San Diego, Biomedical Sciences Building, Room 5090, 9500 Gilman Drive, La Jolla, CA 92093-0635. E-mail address: dbroide@ucsd.edu

Abbreviations used in this article: ADAM8, a disintegrin and metalloproteinase domain–containing protein 8; ATF6, activating transcription factor 6; BAL, bronchoalveolar lavage; ER, endoplasmic reticulum; hORMDL3$^{zp3\text{-}Cre}$, human orosomucoid-like 3 zona pellucida 3 Cre; IP-10, IFN-γ–induced protein 10; Ire1, inositol-requiring enzyme 1; ITAC, IFN-inducible T cell α; MBP, major basic protein; MMP, matrix metalloproteinase; ORMDL, orosomucoid-like; PAS, periodic acid–Schiff; PERK, protein kinase regulated by RNA-like endoplasmic reticulum–associated kinase; RFP, red fluorescent protein; SERCA2b, sarco/endoplasmic reticulum Ca^{2+} ATPase; SNP, single nucleotide polymorphism; Tg, transgenic; UPR, unfolded protein response; zp3, zona pellucida 3; WT, wild-type.

(MMP-9, ADAM8, CCL20, CXCL10, CXCL11) may contribute to the pathogenesis of asthma.

Although our previous studies demonstrated that *Ormdl3* is an allergen and Th2 cytokine–inducible gene that is dependent upon Stat6 for expression (13), these prior studies in WT mice did not determine which downstream pathways were regulated by ORMDL3 in vivo. To address this question we have generated ORMDL3 transgenic (Tg) mice, and in this study we demonstrate that Tg mice overexpressing human ORMDL3 (hORMDL3) spontaneously develop significantly increased levels of airway remodeling (smooth muscle, fibrosis, mucus) that precede the development of airway inflammation. Additionally, allergen challenge of ORMDL3 Tg mice resulted in enhanced OVA-specific IgE responses compared to OVA-challenged WT mice and was associated with increased major basic protein (MBP) positive peribronchial eosinophils and lung levels of IL-4. These studies in ORMDL3 Tg mice also provide evidence that the ER-localized ORMDL3 plays an important role in selective activation of one of the three UPR pathways in vivo (i.e., ATF6), and that expression of ORMDL3 in vivo regulates airway remodeling (smooth muscle, fibrosis, mucus) potentially through ATF6 target genes such as SERCA2b and/or through ATF6-independent genes (TGF-β1, ADAM8), which we detected at increased levels in the lungs of ORMDL3 Tg mice. ORMDL3 may therefore activate several pathways important to the pathogenesis of airway remodeling and asthma in vivo.

Materials and Methods

Zp3-Cre mice

Zp3-*Cre* mice (embryonic *Cre* expression) on a C57BL/6 background were acquired from The Jackson Laboratory.

hORMDL3$^{zp3\text{-}Cre}$ mouse generation

All the mouse experimental protocols were approved by the University of California, San Diego Institutional Animal Care and Use Committee.

Targeting plasmid construction. The hORMDL3 Tg construct pCAGEN Lox red fluorescent protein (RFP)-H2B STOP Lox hORMDL3 was generated by cloning the 462-bp hORMDL3 open reading frame from pCMV6-AC-ORMDL3 (Origene) with AgeI/NotI into a construct previously developed and provided by A.J. Holland and D.W. Cleveland (Ludwig Institute for Cancer Research at the University of California, San Diego, CA).

RFP-Stop^{FL}hORMDL3-Tg mouse generation. SpeI/PvuI-linearized pCAGEN Lox RFP-H2B STOP Lox hORMDL3 (Fig. 1A, 1B) was microinjected into the pronuclei of fertilized mouse embryos and implanted into a pseudopregnant mouse (all on a C57BL/6 background) via an established protocol by the University of California, San Diego mouse Tg core. Progeny were then screened by PCR for the presence of the transgene. Subsequent mouse genotyping was performed using PCR with the following primers: F1-3530, 5′-GCA ACG TGC TGG TTA TTG TG-3′; F2-4009, 5′-CCC CCT GAA CCT GAA ACA TA-3′; R-4644, 5′-TAC AGC ACG ATG GGT GTG AT-3′ (Fig. 1C). These RFP-Stop^{FL} hORMDL3-Tg mice (C57BL/6 background) were crossed with zp3-*Cre* mice (C57BL/6 background) to generate hORMDL3$^{zp3\text{-}Cre}$ mice (C57BL/6 background).

Processing of lungs, bronchoalveolar lavage, and blood

hORMDL3$^{zp3\text{-}Cre}$ mice and littermate controls were euthanized at different ages (4, 8, and 26 wk) to quantitate levels of airway inflammation, airway remodeling, as well as expression of cytokines, chemokines, and remodeling genes. In addition to examining whole lung, purified populations of selected lung cell types (bronchial epithelium, bronchoalveolar lavage [BAL] macrophages) were also studied. Levels of IgE and other Igs were quantitated in peripheral blood.

Lung processing. Lungs were processed for protein and RNA extraction, as well as for immunohistology (paraffin-embedded lung sections) as previously described in this laboratory (13, 16). For protein and RNA extractions, lungs were initially snap-frozen in liquid nitrogen and stored at −80°C. For paraffin-embedded sections, lungs were equivalently inflated with an intratracheal injection of the same volume of 4% paraformaldehyde solution (Sigma-Aldrich, St. Louis, MO) to preserve the pulmonary architecture. Lung sections were processed for immunohistochemistry to detect MBP (anti-mouse MBP Ab was provided by Dr. James Lee, Mayo Clinic, Scottsdale, AZ), neutrophil elastase (anti-mouse neutrophil elastase Ab; Santa Cruz Biotechnology), F4/80 (anti-mouse F4/80 Ab; Santa Cruz Biotechnology), and CD4 (anti-mouse CD4 Ab; GeneTex). The number of individual cells staining positive for different cell types in the peribronchial space was counted using a light microscope. Results are expressed as the number of peribronchial cells staining positive per bronchiole with 150–200 μm internal diameter. At least 10 bronchioles were counted in each slide.

BAL macrophages. In selected experiments, purified populations of BAL macrophages (>98% purity) were obtained by adhesion by placing BAL cells in a 10-cm petri dish in complete media for 4 h at 37°C as previously described in this laboratory (13). Pooled BAL macrophages from four mice per group were used for RNA and protein extraction.

Isolation of bronchial epithelial cells. The isolation of bronchial epithelial cells was performed as previously described in this laboratory (13, 17). Briefly, the epithelial brushing was performed using a sterile plastic feeding tube (Solomon Scientific) inserted into the right main and left main bronchi with gentle brushing and immediately placed in RNA STAT-60 (Tel-Test) for RNA extraction. Bronchial epithelial cells were of >95% purity as assessed by E-cadherin expression on FACS and histologic detection of ciliated epithelial cells (13, 17). Four mice per group were used for each data point.

BAL fluid collection. BAL fluid was collected by lavaging the lung with 1 ml PBS via a tracheal catheter as previously described (16). BAL fluid was centrifuged, and the supernatant frozen at −80°C for subsequent cytokine analysis.

Peripheral blood. Peripheral blood was obtained from mice by cardiac puncture into tubes without anticoagulant added for quantitation of serum Ig levels.

Detection of ORMDL3- and ORMDL3-regulated genes by quantitative RT-PCR

Quantitative RT-PCR was performed as previously described in this laboratory (13). In brief, total RNA was extracted with RNA STAT-60 (Tel-Test) and reverse transcribed with oligo(dT) and SuperScript II kit (Life Technologies). Quantitative PCR was performed with TaqMan PCR Master Mix and ORMDL1, ORMDL2, ORMDL3 (human and mouse), SERCA2b, TGF-β1, ADAM8, MMP-9, ITAC, and IP-10 primers (all from Applied Biosystems). The relative amounts of transcripts were normalized to those of housekeeping gene (GAPDH) mRNA and compared between the different genes by the ΔΔCt method as previously described in this laboratory (13).

Detection of airway remodeling

Peribronchial smooth muscle layer. The thickness of the airway smooth muscle layer was measured by α-smooth muscle actin immunohistochemistry as previously described (16). Lung sections were immunostained with an anti–α-smooth muscle actin primary Ab (Sigma-Aldrich) to detect peribronchial smooth muscle. Species- and isotype-matched Abs were used as controls in place of the primary Ab. The area of peribronchial α-smooth muscle actin staining in paraffin-embedded lungs was outlined and quantified under a light microscope (Leica DMLS, Leica Microsystems) attached to an image analysis system (Image-Pro Plus, Media Cybernetics, Bethesda, MD) as previously described (16). Results are expressed as the area of peribronchial α-smooth muscle actin staining per micrometer length of basement membrane of bronchioles 150–200 μm internal diameter.

Peribronchial trichrome staining. The area of peribronchial trichrome staining in paraffin-embedded lungs was outlined and quantified under a light microscope (Leica DMLS, Leica Microsystems) attached to an image analysis system (Image-Pro Plus, Media Cybernetics) as previously described (16). Results are expressed as the area of trichrome staining per micrometer length of basement membrane of bronchioles 150–200 μm internal diameter.

Lung collagen. The amount of lung collagen was measured as previously described in this laboratory (16) with a collagen assay kit that uses a dye reagent that selectively binds to the [Gly-X-Y]n tripeptide sequence of mammalian collagens (Biocolor, Newtonabbey, U.K.). In all experiments, a collagen standard was used to calibrate the assay.

Airway mucus expression. To quantitate the level of mucus expression in the airway, the number of periodic acid–Schiff (PAS)$^{+}$ and PAS^{-} epithelial cells in individual bronchioles was counted as previously described in this

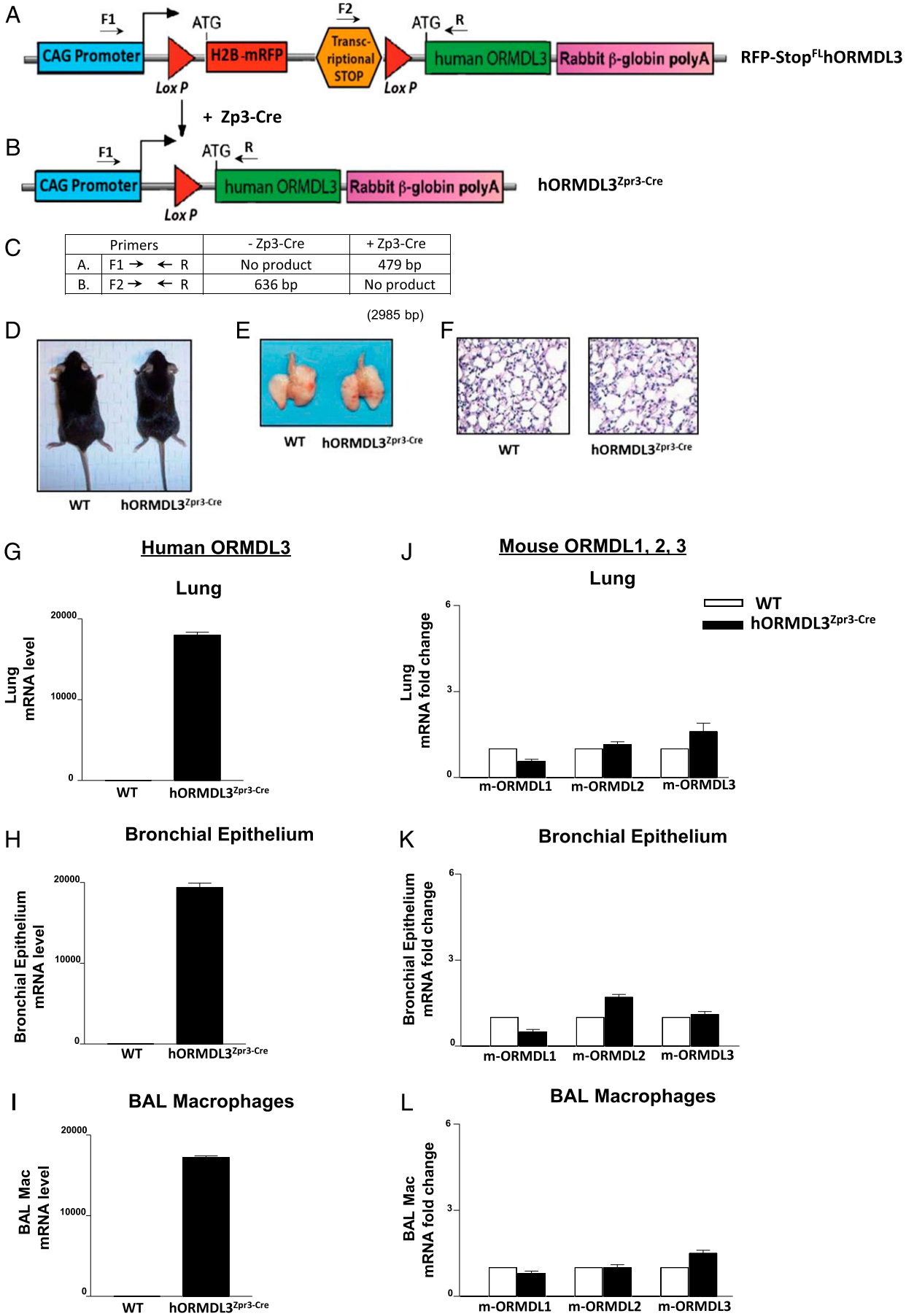

FIGURE 1. Generation of ORMDL3 Tg mice. (**A**) The human ORMDL3 Tg construct contains a CAG promoter for universal overexpression (light blue), H2B-RFP (RFP) (red), followed by a transcriptional stop site (orange), the human ORMDL3 open reading frame (green), and (*Figure legend continues*)

laboratory (16). At least 10 bronchioles were counted in each slide. Results are expressed as the percentage of PAS^+ cells per bronchiole, which is calculated from the number of PAS^+ epithelial cells per bronchus divided by the total number of epithelial cells of each bronchiole.

Lung protein for ELISA and Western blot

Lung tissue was homogenized in 500 μl lysis buffer and 100 mg stainless steel beads (Next Advance) for 5 min using the Bullet Blender homogenizer (Next Advance). The lysate was centrifuged at 13,000 rpm for 10 min at 4°C. The supernatant was used for ELISA and Western blots.

Quantitation of lung cytokines

BAL fluid and lung levels of selected Th2 cytokines (IL-4, IL-5, IL-13) and chemokines (eotaxin-1) was performed by ELISA according to the manufacturer's instructions (R&D Systems). Levels of lung IL-4, IL-5, IL-13, and eotaxin-1 are expressed as the amount of cytokine/chemokine in picograms per milligram lung protein. Lung protein levels were quantitated by the bicinchoninic acid method (Thermo Scientific).

Detection of SERCA2b by Western blot

Lung protein was separated on an SDS-PAGE gel and transferred to a polyvinylidene difluoride membrane. Membranes were blocked in 5% (w/v) milk in 1× Tris-buffered saline with Tween 20 for 1 h and then incubated with the primary Ab overnight at 4°C. The primary Abs used in this study were mouse monoclonal anti-SERCA2b (Abcam) and rabbit monoclonal anti-GAPDH (Genetex).

Quantitation of bronchial epithelial TGF-β1, ADAM8, SERCA2b and MMP-9 by image analysis

Lung sections from $hORMDL3^{zp3\text{-}Cre}$ and WT mice were immunostained with either anti–TGF-β1, anti-ADAM8, SERCA2b, or anti–MMP-9 Abs. Levels of expression of either TGF-β1, ADAM8, SERCA2b, or MMP-9 by bronchial epithelial cells (outlined and visualized with a light microscope attached to an image analysis system) were quantitated by image analysis as described (18). The images were saved and analyzed with Image-Pro Plus 3 software (Media Cybernetics). The mean value of bronchial epithelial immunostaining intensity was normalized for the total area of bronchial epithelium.

Quantitation of serum IgE, IgG, IgM, and IgA

Serum total IgE was quantitated with an IgE ELISA kit (BD Biosciences). Serum IgG (IgG1 and IgG2a), IgM, and IgA were quantitated using a mouse Ig isotyping ELISA kit (BD Pharmingen) with results reported as OD at 450 nm per the manufacturer's instructions. Serum OVA-specific IgE was quantitated with a mouse OVA-specific IgE kit (BioLegend) with results reported as nanograms per milliliter. All ELISA plates were read with a Bio-Rad model 680 microplate reader.

Activation of ATF6, Ire1, and PERK

Purified populations of macrophages (>95% pure) were generated from $hORMDL3^{zp3\text{-}Cre}$ and WT mouse bone marrow cells cultured in complete DMEM media (Gibco) supplemented with stem cell growth factors (L Cells media, American Type Culture Collection) for 10 d as described (19). Activation of ATF6 was detected with immunofluorescence microscopy to detect nuclear localization of ATF6 using an ATF6 Ab (Imgenex) as previously described (13, 20). Activation of inositol-requiring enzyme 1 (Ire1) was detected by PCR, as it removes the UPR intron from the unspliced form of XBP1 to generate the spliced form of XBP1 mRNA (13, 20). Activation of protein kinase regulated by RNA-like endoplasmic reticulum–associated kinase (PERK) was assessed by increased levels of phospho-eIF2α by Western blot using an Ab specific to the phosphorylated form of eIF2α (13, 20). In all UPR experiments, thapsigargin, a known activator of the UPR, was incubated with cells for 1 h before collecting cells for either RNA or protein analyses. Because insufficient numbers of bronchial epithelial cells were available for UPR Western blot studies, the UPR studies were performed on macrophages, a cell type that similar to epithelial cells expresses high levels of ORMDL3 (13).

Acute OVA challenge model

$hORMDL3^{zp3\text{-}Cre}$ and littermate control mice aged 12 wk were sensitized and challenged with OVA (Worthington, Lakewood, NJ) as previously described (13). In brief, mice were sensitized i.p. with 100 μg OVA and 2 mg aluminum hydroxide (Imject Alum; Thermo Fisher Scientific, Waltham, MA) in a total volume of 200 μl PBS on days 0 and 10 followed by intranasal administration of 200 μg OVA in 20 μl PBS on days 21, 23, and 25. Non–OVA-challenged ORMDL3 Tg and littermate groups of mice were sensitized and challenged with PBS only. Twenty-four hours after the last challenge, BAL fluid, lungs, and blood were collected as described above.

Airway hyperreactivity to methacholine.

Airway responsiveness to methacholine was assessed in intubated and ventilated mice aged 12 wk (n = 8 mice/group) (flexiVent ventilator; Scireq) anesthetized with ketamine (100 mg/kg) and xylazine (10 mg/kg) i.p. as previously described (16). The dynamic airway resistance and elastance were determined using Scireq software in mice exposed to nebulized PBS and methacholine (0, 3, 24, and 48 mg/ml). The following ventilator settings were used: tidal volume (10 ml/kg), frequency (150/min), and positive end-expiratory pressure (3 cmH_2O). Increased elastance values signal an increased stiffness of the lungs, and elastance is the inverse of compliance (Scireq).

Statistical analysis

All results are presented as means ± SEM. A statistical software package (GraphPad Prism; GraphPad Software, San Diego, CA) was used for the analysis. A p value <0.05 was considered statistically significant.

Results

Generation of hORMDL3 Tg mice

To perform studies in hORMDL3 Tg mice, we generated conditional hORMDL3 Tg floxed mice (RFP-$Stop^{FL}$hORMDL3-Tg mice) with the pCAGEN lox RFP-H2B STOP lox hORMDL3 transgene construct (Fig. 1A, 1B), and crossed these with zona pellucida 3 (zp3) Cre mice, resulting in offspring with expression of human ORMDL3 in all cells ($hORMDL3^{zp3\text{-}Cre}$ mice) (21). The transgene construct we developed has a loxP-flanked RFP and transcriptional stop codon positioned at the transcriptional initiation site of the hORMDL3 transgene which prevents transcription of hORMDL3 (Fig. 1A). Thus, all cells in this RFP-$Stop^{FL}$ hORMDL3-Tg mouse will not express hORMDL3 until crossed with a Cre-expressing mouse, which excises the transcriptional stop codon and RFP (Fig. 1B). We used PCR (Fig. 1C) to confirm successful expression of the hORMDL3 transgene in $hORMDL3^{zp3\text{-}Cre}$ mice. The presence of the nonexpressed floxed transgene construct in RFP-$Stop^{FL}$hORMDL3-Tg mice tissues/cells was assessed by red

a rabbit β-globin polyadenylation sequence (pink). The H2B-RFP (RFP) and transcriptional stop site are flanked by LoxP sites (triangles). Cells containing this pCAGEN Lox RFP-H2B STOP Lox hORMDL3 construct will express RFP and not express hORMDL3, as the transcriptional stop codon (orange) prevents transcription of hORMDL3. (**B**) Expression of the hORMDL3 gene is Cre recombinase–dependent because the transcriptional stop codon preventing hORMDL3 expression (and RFP) are excised by Cre recombinase via the Lox P sites resulting in overexpression of hORMDL3 only in those cells expressing Cre recombinase. (**C**) Primer sets (F1, R; F2, R) used to detect progeny of RFP-$Stop^{FL}$hORMDL3-Tg mice crossed with zp3-Cre mouse and predicted sizes of transgene mRNA assessed by PCR. (**D**) WT mice (*left*) and $hORMDL3^{zp3\text{-}Cre}$ mice (*right*) aged 26 wk appeared morphologically similar. (**E**) The gross appearance of lungs of WT mice (*left*) and $hORMDL3^{zp3\text{-}Cre}$ mice (*right*) aged 26 wk appeared morphologically similar. (**F**) Other than airway remodeling, the appearance of lungs of WT mice (*left*) and $hORMDL3^{zp3\text{-}Cre}$ mice (*right*) aged 26 wk appeared morphologically similar. Original magnification ×200. (**G**) Expression of the hORMDL3 transgene was detected by quantitative RT-PCR in mouse lung, (**H**) mouse bronchial epithelium, and (**I**) mouse BAL macrophages in $hORMDL3^{zp3\text{-}Cre}$ mice, but not in WT mice. The hORMDL3 transgene did not increase levels of mouse ORMDL1 (mORMDL1), mouse ORMDL2 (mORMDL2), or mouse ORMDL3 (mORMDL3) as assessed by quantitative RT-PCR in mouse lung (**J**), mouse bronchial epithelium (**K**), and mouse BAL macrophages (**L**) in either $hORMDL3^{zp3\text{-}Cre}$ or WT mice.

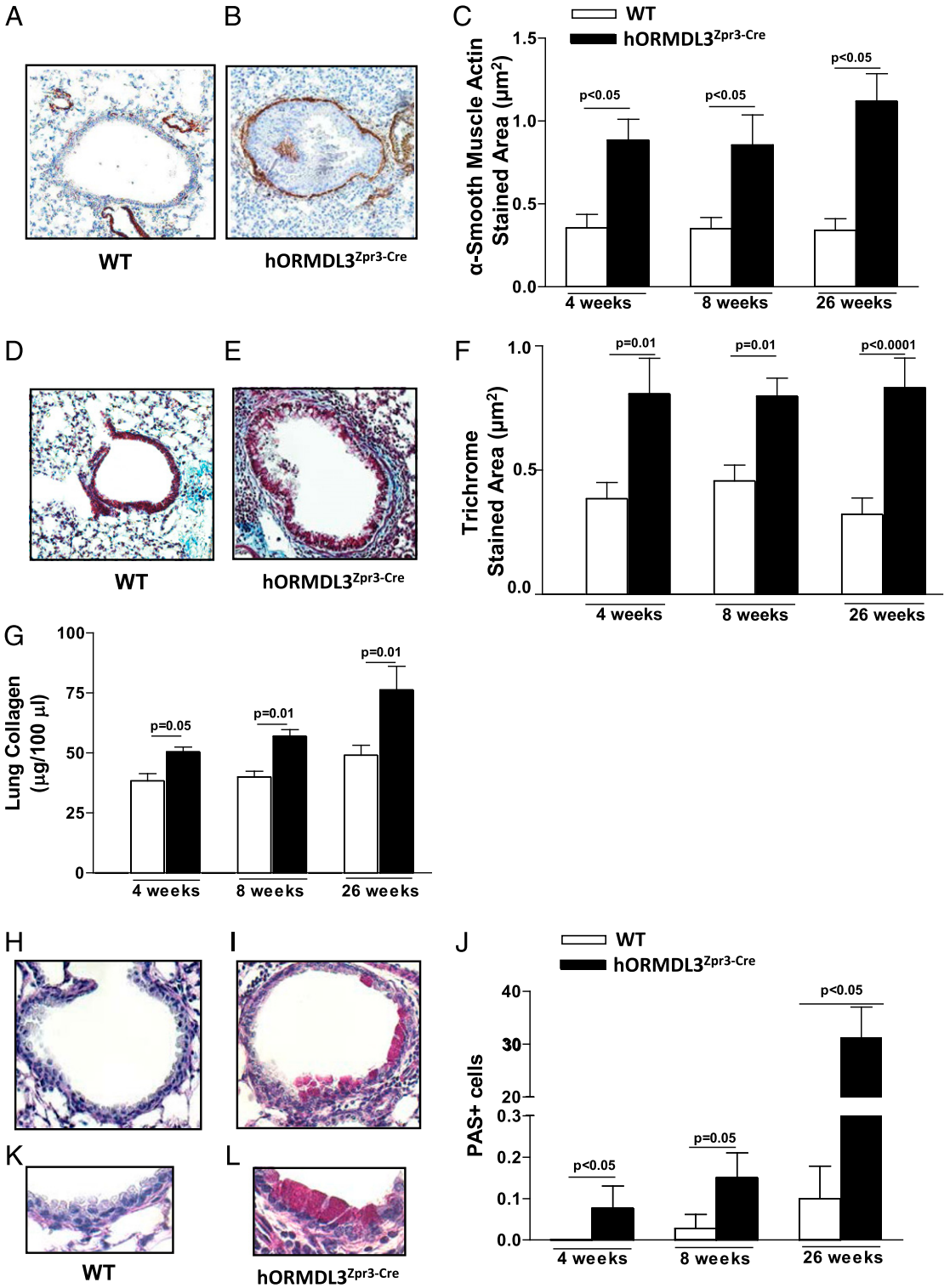

FIGURE 2. Airway remodeling in hORMDL3$^{zp3\text{-}Cre}$ mice. (**A**–**C**) Levels of peribronchial smooth muscle were quantitated by immunohistochemistry using an anti–α-smooth muscle actin Ab and image analysis. Results are expressed as the α-smooth muscle actin stained area (square micrometers) per micrometer length of basement membrane of bronchioles 150–200 μm internal diameter in (A) WT and (B, C) hORMDL3$^{zp3\text{-}Cre}$ mice at 4, 8, and 26 wk of age (n = 12 mice/group). (**D**–**F**) Levels of peribronchial trichrome staining were quantitated by image analysis. Results are expressed as the trichrome-stained area (square micrometers) per micrometer length of basement membrane of bronchioles 150–200 μm internal diameter in (D) WT and (E, F) hORMDL3$^{zp3\text{-}Cre}$ mice 4, 8, and 26 wk of age (n = 12 mice/group). (**G**) Levels of lung collagen were quantitated by a Sircol assay in WT and hORMDL3$^{zp3\text{-}Cre}$ mice at 4, 8, and 26 wk of age (n = 12 mice/group). (**H**–**L**) Levels of mucus were quantitated by PAS staining in (H) WT and (I, J) hORMDL3$^{zp3\text{-}Cre}$ mice at 4, 8, and 26 wk of age (n = 12 mice/group). Higher magnification view of PAS staining in (K) WT and (L) hORMDL3$^{zp3\text{-}Cre}$ mice. (A, B, D, E, H, and I) Original magnification ×200. (K and L) Original magnification ×400.

fluorescence prior to crossing to zp3 Cre mice. Crossing RFP-Stop^{FL} hORMDL3-Tg mice to zp3 Cre mice results in the loss of RFP expression in cells that were designed to provide a rapid initial screen for successful expression of hORMDL3 (Fig. 1A, 1B). However, because levels of the RFP as detected by immunofluorescence microscopy varied widely in RFP-Stop^{FL}hORMDL3-Tg mice, we utilized hORMDL3 PCR, rather than loss of red fluoresecence, to detect hORMDL3 expression. hORMDL3$^{zp3\text{-}Cre}$ mice overexpressing hORMDL3 constitutively in all cells were viable with no obvious developmental or morphologic defects (Fig. 1D), and their lung size and weights and were similar to those of WT mice (Fig. 1E, 1F).

Levels of the human ORMDL3 transgene were highly expressed in hORMDL3$^{zp3\text{-}Cre}$ mouse lung (Fig. 1G), bronchial epithelium (Fig. 1H), and BAL macrophages (Fig. 1I) as assessed by quantitative RT-PCR. In contrast, no expression of the human ORMDL3 transgene was detected in WT littermate mice (referred to as WT subsequently) (Fig. 1G–I). Levels of mouse ORMDL1, mouse ORMDL2, and mouse ORMDL3 in hORMDL3$^{zp3\text{-}Cre}$ mice were not altered in mouse lung (Fig. 1J), bronchial epithelium (Fig. 1K), and BAL macrophages (Fig. 1L) as assessed by quantitative RT-PCR.

Increased airway remodeling in hORMDL3$^{zp3\text{-}Cre}$ mice

hORMDL3$^{zp3\text{-}Cre}$ mice have evidence of airway remodeling characteristic of asthma at 4 wk of age, which persisted through 26 wk of life (Fig. 2). Features of airway remodeling that are evident in hORMDL3$^{zp3\text{-}Cre}$ mice include an increase in the area of peribronchial smooth muscle as assessed by immunostaining with an anti–α-smooth muscle actin Ab (Fig. 2A–C), an increase in peribronchial fibrosis as assessed by the area of peribronchial trichrome staining to detect lung collagen (Fig. 2D–F), and an increase in total lung collagen (Fig. 2G). Additionally, there was a significant increase in mucus expression detected by PAS staining (Fig. 2H–L). Although the levels of peribronchial smooth muscle (Fig. 2C) and peribronchial fibrosis as assessed by trichrome staining (Fig. 2F) remained stably increased from week 4 to week 26, levels of mucus continued to increase from week 4 to week 26 (Fig. 2J).

Activation of ATF6 but not Ire1 or PERK in hORMDL3$^{zp3\text{-}Cre}$ mice

We have previously demonstrated that in vitro transfection of ORMDL3 activates only one of the three pathways of the UPR (i.e., activates the ATF6 pathway and not the Ire1 or PERK pathway) (13). To determine whether in vivo hORMDL3 activated the UPR, we cultured bone marrow–derived macrophages from WT and hORMDL3$^{zp3\text{-}Cre}$ mice to have sufficient numbers of cells to perform a Western blot. hORMDL3$^{zp3\text{-}Cre}$ mouse macrophages, but not WT macrophages, spontaneously activated the ATF6 pathway as assessed by translocation of ATF6 from being dispersed in the ER to the nucleus using immunofluorescence microscopy (Fig. 3A, 3B). In contrast, both WT and hORMDL3$^{zp3\text{-}Cre}$ mouse macrophages did not activate either Ire1 (Fig. 3C) or PERK (Fig. 3D) pathways. Incubation of WT and hORMDL3$^{zp3\text{-}Cre}$ mouse macrophages with thapsigargin, a known activator of the UPR, induced activation of the ATF6 (Fig. 3A, 3B), Ire1 (Fig. 3C), and PERK (Fig. 3D) pathways in both WT and hORMDL3$^{zp3\text{-}Cre}$ mouse macrophages. Thus, bone marrow–derived macrophages

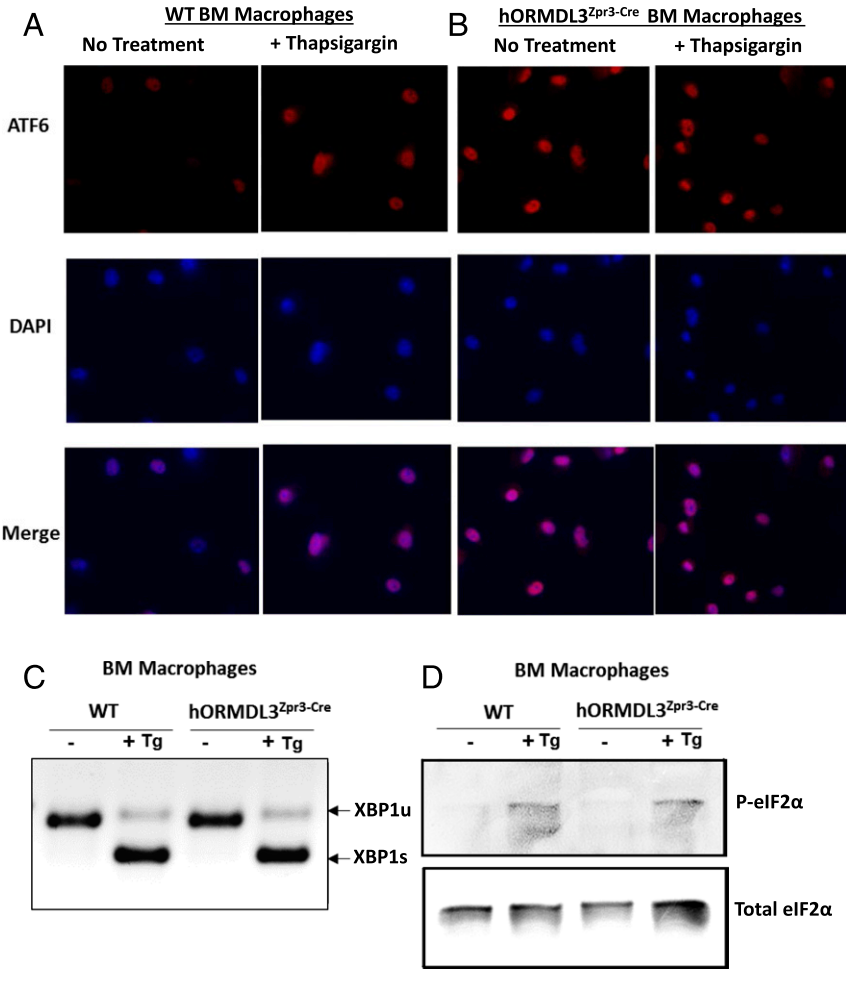

FIGURE 3. ORMDL3 and UPR. Bone marrow–derived macrophages from WT or hORMDL3$^{zp3\text{-}Cre}$ mice were treated with thapsigargin (TG), a known activator of the UPR, for 1 h. (**A** and **B**) ATF6. Immunofluorescence against ATF6 (red) was performed. Active ATF6 is shown by nuclear localization (merged purple color) as depicted by colocalization with DAPI (blue). Original magnification ×400. (**C**) Ire1. Activation of Ire1 was detected by RT-PCR, as it removes the UPR intron from the unspliced form of XBP1 (XBP1u) to generate the spliced form of XBP1 (XBP1s) mRNA. (**D**) PERK. Activation of PERK is assessed by phosphorylation of eIF2α (P-eIF2α) blotted by anti–phospho-specific eIF2α Ab on SDS-PAGE by Western blot. Total eIF2α was blotted by anti-eIF2α Ab.

from hORMDL3$^{zp3\text{-}Cre}$ mice, similar to cells transfected with ORMDL3 in vitro (13), exhibit selective activation of the ATF6 UPR pathway.

Increased remodeling genes in lungs of hORMDL3$^{zp3\text{-}Cre}$ mice

Because SERCA2b has been implicated in airway remodeling in asthma (15), we examined whether levels of SERCA2b were modulated in hORMDL3$^{zp3\text{-}Cre}$ mice. Our studies demonstrate that hORMDL3$^{zp3\text{-}Cre}$ mice have increased lung levels of SERCA2b as assessed by quantitative RT-PCR (Fig. 4A) and Western blot (Fig. 4B). Additionally, hORMDL3$^{zp3\text{-}Cre}$ mice have increased levels of bronchial epithelial expression of TGF-β1 (Fig. 4C) and ADAM8 (Fig. 4D), with a smaller increase in MMP-9 (Fig. 4E) as assessed by quantitative RT-PCR. Levels of TGF-β1 (Fig. 4F), ADAM8 (Fig. 4G), and SERCA2b (Fig. 4H), but not MMP-9 (data not shown), were increased in bronchial epithelium in

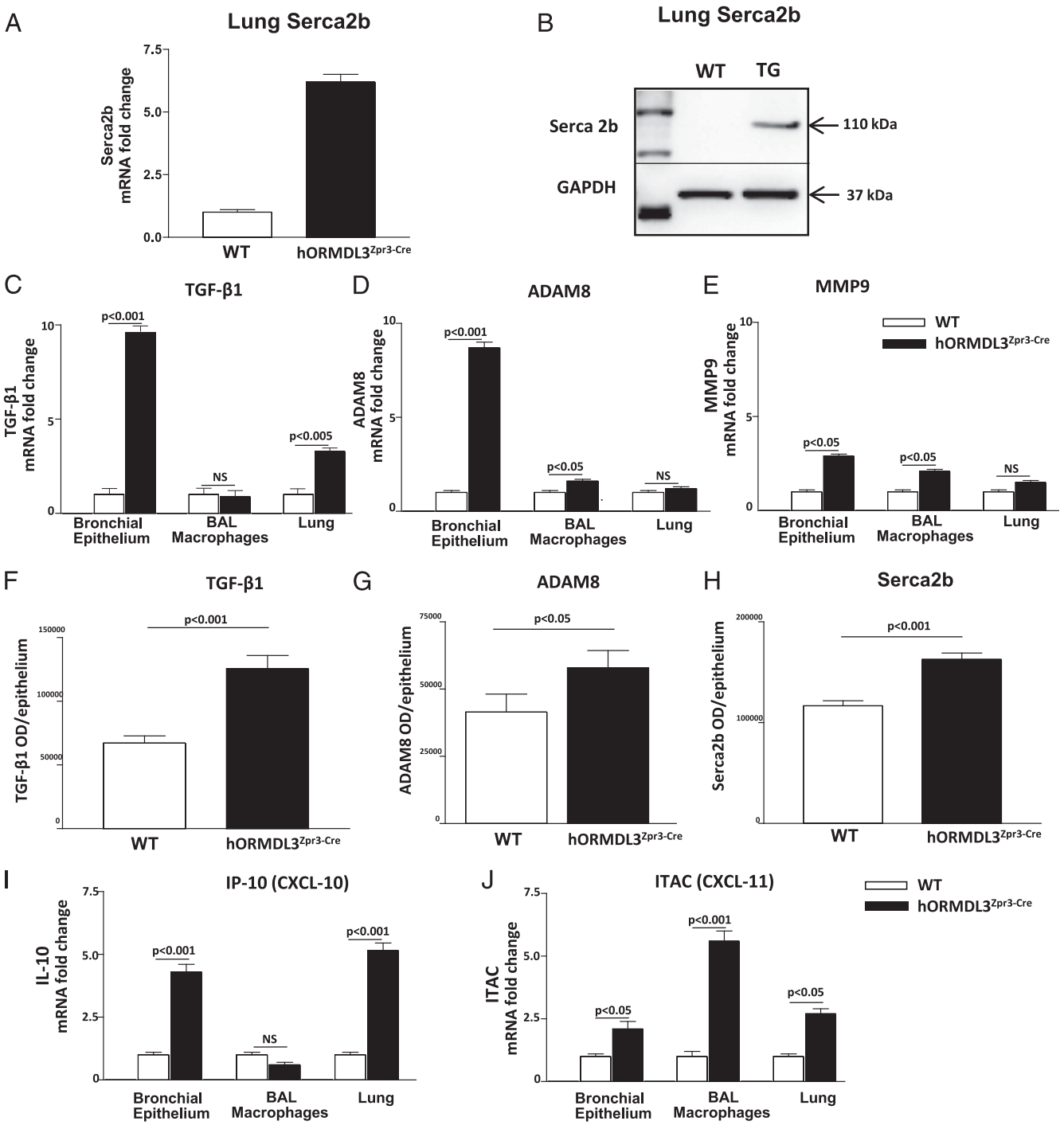

FIGURE 4. hORMDL3$^{zp3\text{-}Cre}$ mice express SERCA2b, TGF-β1, ADAM8, MMP-9, CXCL10, and CXCL11. Levels of SERCA2b were quantitated in the lungs of hORMDL3$^{zp3\text{-}Cre}$ and WT mice by (**A**) quantitative PCR and (**B**) Western blot. Levels of (**C**) TGF-β1, (**D**) ADAM8, and (**E**) MMP-9 were quantitated by quantitative PCR in the lungs, bronchial epithelium, and BAL macrophages of hORMDL3$^{zp3\text{-}Cre}$ and WT mice. Levels of (**F**) TGF-β1, (**G**) ADAM8, and (**H**) SERCA2b were quantitated by immunohistochemistry and image analysis in bronchial epithelium of hORMDL3$^{zp3\text{-}Cre}$ and WT mice. Levels of (**I**) CXCL10 (IP-10) and (**J**) CXCL11 (ITAC) were quantitated by quantitative PCR in the lungs, bronchial epithelium, and BAL macrophages of hORMDL3$^{zp3\text{-}Cre}$ and WT mice (n = 12 mice/group).

hORMDL3$^{zp3\text{-}Cre}$ mice as assessed by immunohistochemistry with quantitation by image analysis.

Levels of selected CXC and CC chemokines in hORMDL3$^{zp3\text{-}Cre}$ mice

Because we had previously demonstrated that transfection of ORMDL3 in vitro induced high levels of expression of CXC chemokines (IL-8; CXCL10, also known as IP-10; CXCL11, also known as ITAC) (13) and lower levels of CC chemokines (CCL20, also known as MIP-3α) (13), we measured levels of these chemokines by quantitative PCR in the hORMDL3$^{zp3\text{-}Cre}$ mice. hORMDL3$^{zp3\text{-}Cre}$ mice had significantly increased levels of lung CXC chemokine mRNA, including CXCL10 in bronchial epithelial cells (Fig. 4I), as well as increased levels of CXCL11 mRNA in BAL macrophages (Fig. 4J), whereas levels of lung KC mRNA, the murine equivalent of IL-8, was not increased (data not shown). Levels of selected CC chemokine mRNA (CCL20 and eotaxin-1) were also not different in lung, bronchial epithelium, or BAL macrophages in hORMDL3$^{zp3\text{-}Cre}$ compared to WT mice (data not shown).

Airway remodeling preceded airway inflammation in hORMDL3$^{zp3\text{-}Cre}$ mice

hORMDL3$^{zp3\text{-}Cre}$ mice exhibit significant airway remodeling at 4 wk of age (Fig. 2), a time point at which there is no evidence of any increase in peribronchial CD4$^+$ cells (Fig. 5A), F4/80$^+$ macrophages (Fig. 5B), MBP$^+$ eosinophils (Fig. 5C), or neutrophil elastase$^+$ neutrophils (Fig. 5D) compared to WT mice. At 8 wk of age there is a small increase in F4/80$^+$ peribronchial macrophages (Fig. 5B) in the lungs of hORMDL3$^{zp3\text{-}Cre}$ mice, with no change in CD4$^+$ cells, eosinophils, or neutrophils (Fig. 5A, 5C, 5D). At 26 wk of age there is a significant increase in peribronchial CD4$^+$ cells (Fig. 5A),

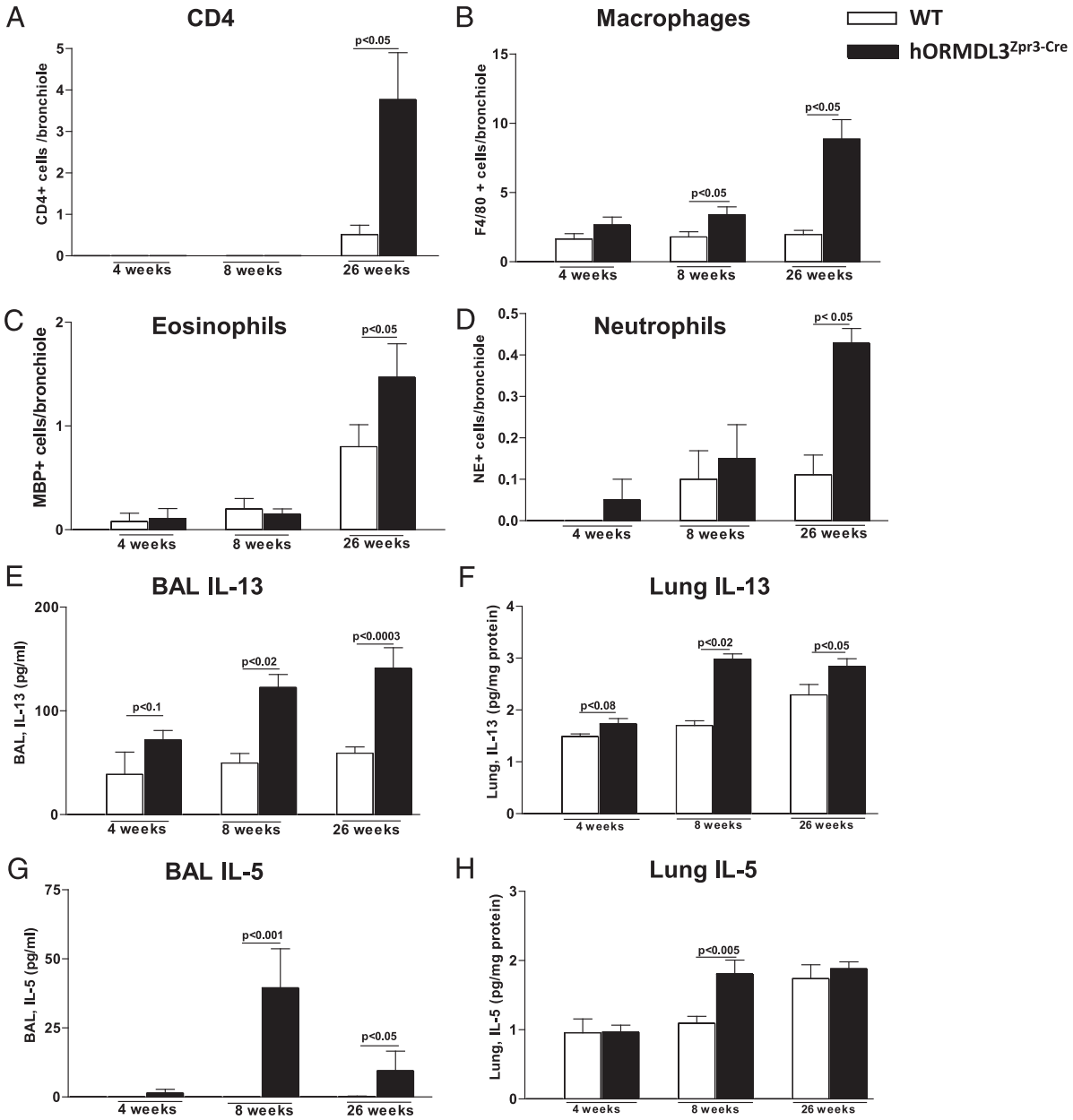

FIGURE 5. Levels of lung immune and inflammatory cells, and Th2 cytokines in hORMDL3$^{zp3\text{-}Cre}$ mice. The number of (**A**) CD4$^+$, (**B**) F4/80$^+$, (**C**) MBP$^+$, and (**D**) neutrophil elastase$^+$ (NE$^+$) cells per bronchiole of 150–200 μm internal diameter was quantitated by immunohistochemistry and image analysis in WT and hORMDL3$^{zp3\text{-}Cre}$ mice at 4, 8, and 26 wk of age (n = 12 mice/group). Levels of IL-13 in (**E**) BAL and (**F**) lung, as well as levels of IL-5 in (**G**) BAL and (**H**) lung, were quantitated by ELISA (n = 12 mice/group).

F4/80^{+} macrophages (Fig. 5B), eosinophils (Fig. 5C), and neutrophils (Fig. 5D) in hORMDL3$^{zp3\text{-}Cre}$ compared to WT mice.

Airway remodeling precedes increase in Th2 cytokines in hORMDL3$^{zp3\text{-}Cre}$ mice

Levels of Th2 cytokines IL-5 and IL-13 were not increased in either BAL or lung of hORMDL3$^{zp3\text{-}Cre}$ mice at 4 wk of age (Fig. 5E–H), a time point at which hORMDL3$^{zp3\text{-}Cre}$ mice exhibit significant airway remodeling. Levels of BAL IL-13 (Fig. 5E) and lung IL-13 (Fig. 5F) were significantly increased in hORMDL3$^{zp3\text{-}Cre}$ mice at 8 and 26 wk of age as assessed by ELISA. Levels of BAL IL-5 (Fig. 5G) were significantly increased in hORMDL3$^{zp3\text{-}Cre}$ mice at 8 and 26 wk of age, whereas levels of lung IL-5 were only increased at 8 wk (Fig. 5H). In contrast, there was no increase in levels of lung IL-4 in hORMDL3$^{zp3\text{-}Cre}$ mice at 4, 8, or 26 wk of age (data not shown).

Increased IgE but not IgG, IgM, or IgA in hORMDL3$^{zp3\text{-}Cre}$ mice

Levels of IgE were significantly increased in hORMDL3$^{zp3\text{-}Cre}$ compared to WT mice at 4 wk of age, and this increase in IgE persisted at 8 and 26 wk (Fig. 6A). The increase in IgE was selective, as there was no increase in IgG (IgG1 or IgG2) (Fig. 6B, 6C), IgM (Fig. 6D), or IgA (Fig. 6E) in hORMDL3$^{zp3\text{-}Cre}$ mice.

Acute OVA allergen challenge enhances peribronchial eosinophilic inflammation, OVA specific IgE, and IL-4 in hORMDL3$^{zp3\text{-}Cre}$ mice

Acute OVA challenge induced a greater increase in peribronchial eosinophils (Fig. 7A–E) and OVA-specific IgE (Fig. 7F) in hORMDL3$^{zp3\text{-}Cre}$ mice compared to WT mice. This was associated with increased lung IL-4 levels in hORMDL3$^{zp3\text{-}Cre}$ mice compared to WT mice (Fig. 7G). Whereas acute OVA challenge induced increased levels of lung IL-5 (Fig. 7I), IL-13 (Fig. 7H), and eotaxin-1 (Fig. 7J) in hORMDL3$^{zp3\text{-}Cre}$ mice (OVA versus no OVA), these levels were not different from those detected in OVA-challenged WT mice.

Airway hyperreactivity to methacholine

hORMDL3$^{zp3\text{-}Cre}$ mice had spontaneously increased airway responsiveness to methacholine compared to WT mice at 12 wk of age (Fig. 8A). Additionally, hORMDL3$^{zp3\text{-}Cre}$ mice had increased lung elastance compared to WT mice (Fig. 8B).

Discussion

Although multiple genetic association studies have demonstrated that ORMDL3 is highly linked to asthma (1–10), the mechanism by which ORMDL3 may contribute to the pathogenesis of asthma in vivo is at present unknown. In this study using a mouse model in which the human *ORMDL3* gene is overexpressed, we demonstrate the novel findings that expression of the human ORMDL3 transgene in vivo is associated with significantly increased airway remodeling, including increased airway smooth muscle, subepithelial fibrosis, and mucus. These airway remodeling changes in hORMDL3$^{zp3\text{-}Cre}$ mice were associated with the spontaneous development of increased airway responsiveness. Additionally, the remodeling changes were associated with an increased lung elastance (the inverse of lung compliance), which indicates an increased stiffness of the remodeled lungs. The mechanism of the increased airway remodeling did not appear to be dependent on increased airway inflammation, as significant airway remodeling was evident at 4 wk of age in the hORMDL3$^{zp3\text{-}Cre}$ mice, a time point not associated with an increased number of peribronchial eosinophils, neutrophils, macrophages, or CD4 cells. Increased levels of expression of genes associated with airway remodeling were detected in the lung (SERCA2b) and airway epithelium (TGF-β1, ADAM8, MMP-9) of hORMDL3$^{zp3\text{-}Cre}$ mice, suggesting that these pathways may contribute to airway remodeling detected in these mice. The importance of these genes that are highly expressed in hORMDL3$^{zp3\text{-}Cre}$ mice to airway remodeling

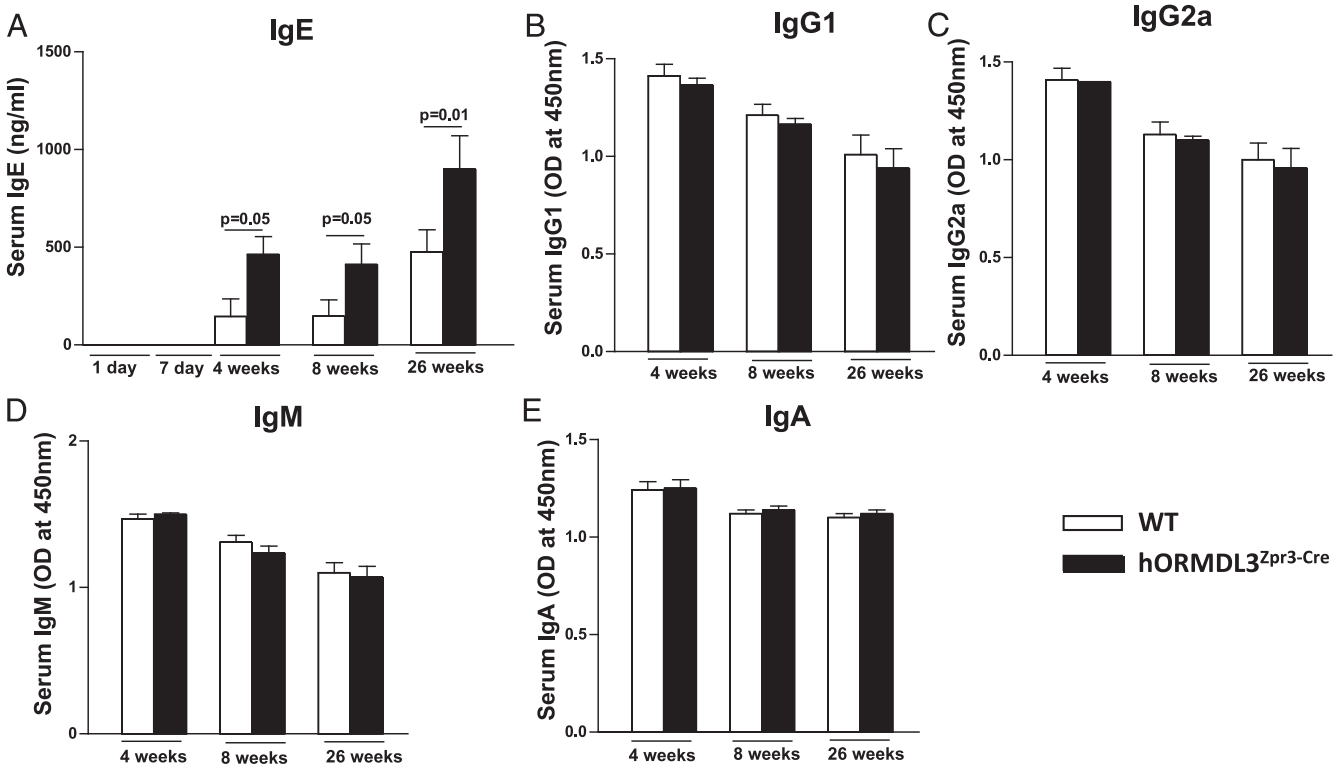

FIGURE 6. Levels of IgE, IgG, IgM, and IgA in hORMDL3$^{zp3\text{-}Cre}$ mice. Levels of (**A**) IgE, (**B**) IgG1, (**C**) IgG2, (**D**) IgM, and (**E**) IgA were quantitated by ELISA in hORMDL3$^{zp3\text{-}Cre}$ (filled bar) and WT (open bar) mice at 4, 8, and 26 wk of age (n = 12 mice/group).

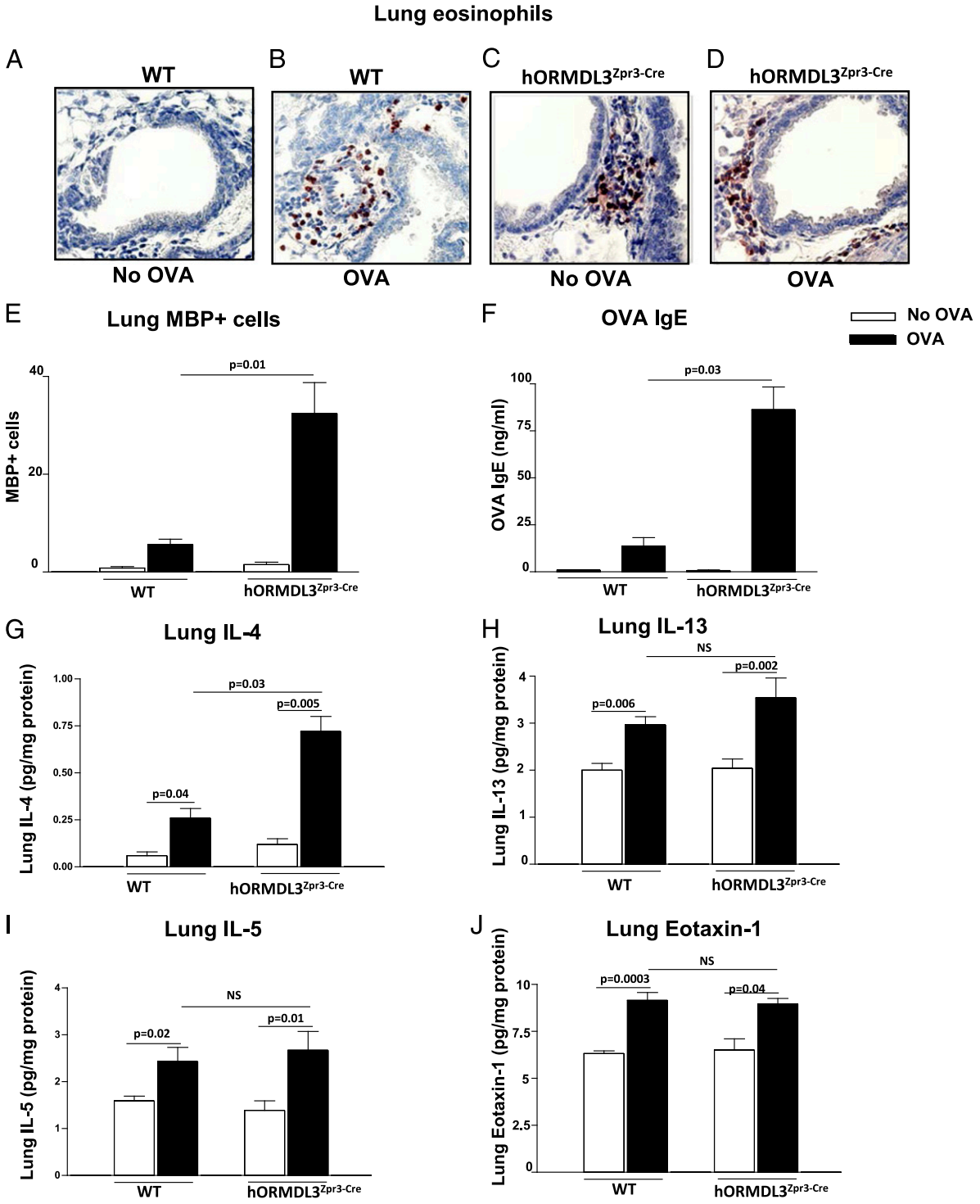

FIGURE 7. Effect of acute OVA allergen challenge on airway inflammation, IgE, and Th2 cytokines in hORMDL3$^{zp3\text{-}Cre}$ mice. hORMDL3$^{zp3\text{-}Cre}$ and WT mice were sensitized to OVA and challenged with OVA allergen by inhalation. Compared to OVA-challenged WT mice, OVA-challenged hORMDL3$^{zp3\text{-}Cre}$ mice had significantly increased levels of (**A**–**E**) lung MBP^{+} peribronchial eosinophils as assessed by immunohistochemistry, (**F**) OVA-specific IgE, and (**G**) lung IL-4. Levels of lung (**H**) IL-13, (**I**) IL-5, and (**J**) eotaxin-1 were similar in OVA-challenged WT and OVA-challenged hORMDL3$^{zp3\text{-}Cre}$ mice (n = 12 mice/group). (A–D) Original magnification ×200.

and asthma is suggested from studies demonstrating expression of these pathways in the airways of human asthmatics (15, 22–27), induction of these mediators by allergen inhalation in asthmatics (TGF-β1, MMP-9) (28–30), and inhibition of asthma outcomes in mice deficient in these genes (ADAM8, Smad3, MMP-9) (31–35), or in mice treated with neutralizing Abs (TGF-β1) (36).

We have previously performed in vitro studies and demonstrated that transfection of ORMDL3 induces activation of one of the three pathways of the ER UPR, namely the ATF6 pathway (13). Using hORMDL3$^{zp3\text{-}Cre}$ mice we have made the novel observation that the ATF6 pathway of the UPR is selectively activated by the human ORMDL3 transgene in vivo. ATF6 (consisting of the closely related ATF6α and ATF6β in mammals) (37) is a transcription factor known to regulate genes involved in ER protein folding (14), as well as expression of SERCA2b, which has been implicated in airway remodeling in asthma (15). In this study we

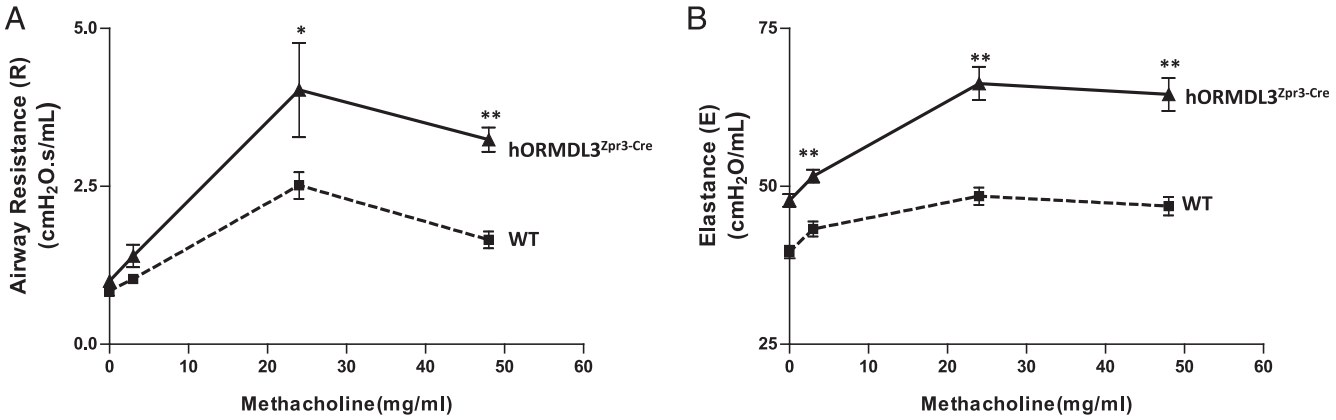

FIGURE 8. Airway responsiveness in hORMDL3$^{zp3\text{-}Cre}$ mice. Airway responsiveness to methacholine (MCh) was assessed in intubated and ventilated hORMDL3$^{zp3\text{-}Cre}$ and WT mice aged 12 wk (flexiVent ventilator; Scireq) (n = 8 mice/group) (**A**). Lung elastance (the inverse of compliance) was also recorded in hORMDL3$^{zp3\text{-}Cre}$ and WT mice (n = 8 mice/group) (**B**). *$p < 0.01$, **$p < 0.002$

demonstrate that hORMDL3$^{zp3\text{-}Cre}$ mice exhibit both activation of ATF6 and increased levels of lung SERCA2b, suggesting that the ATF6 and SERCA2b pathways are downstream of ORMDL3 in vivo as previously demonstrated in vitro (13). In prior in vitro studies we have demonstrated that transfection of ORMDL3 induced activation of ATF6 and expression of SERCA2b, whereas knockdown of ATF6α inhibited SERCA2b expression (13). Activation of ATF6 was maximal, as further induction of the UPR upon treatment of the cells with thapsigargin, a well-characterized ER stress inducer, did not increase the nuclear localization of ATF6. Overall, these studies of hORMDL3$^{zp3\text{-}Cre}$ mice provide in vivo evidence of ATF6α-dependent pathways (SERCA2b) and ATF6α-independent pathways (TGF-β1, ADAM8, MMP-9) through which the ER-localized ORMDL3 may be linked to airway remodeling and asthma. However, only future studies in which the ATF6 pathway is selectively inhibited will be able to determine the role played by the ATF6 pathway in any remodeling changes we have noted in hORMDL3$^{zp3\text{-}Cre}$ mice.

hORMDL3$^{zp3\text{-}Cre}$ mice also had an age-related increase in levels of airway inflammation, as well as an increase in lung cytokines and chemokines. The increased levels of airway inflammation were not evident in hORMDL3$^{zp3\text{-}Cre}$ mice aged 4 wk, and only started to be evident at 8 wk (increase in peribronchial macrophages). At 26 wk hORMDL3$^{zp3\text{-}Cre}$ mice had significantly increased levels of peribronchial CD4$^+$ cells, eosinophils, macrophages, and neutrophils, suggesting that the airway inflammatory response in hORMDL3$^{zp3\text{-}Cre}$ mice increased during the period from 8 to 26 wk of age. Because the inflammatory response in hORMDL3$^{zp3\text{-}Cre}$ mice had evidence of both Th2-mediated inflammation (increased CD4$^+$ cells and eosinophils), as well as increased neutrophils and macrophages, we investigated whether their lungs expressed cytokines and chemokines associated with Th2-mediated inflammation (IL-4, IL-5, IL-13, eotaxin-1) or chemokines known to be regulated by ORMDL3 in vitro (CXCL10, CXCL11, IL-8, CCL20) (13). Levels of lung Th2 cytokines (IL-5 and IL-13) were increased in hORMDL3$^{zp3\text{-}Cre}$ mice at 8 and 26 wk of age. In contrast, there was no increase in lung IL-4 or eotaxin-1 at any time point. Allergen-challenged hORMDL3$^{zp3\text{-}Cre}$ mice had significantly increased levels of peribronchial eosinophils and lung IL-4 compared to allergen-challenged WT mice. IL-4 can contribute to increased lung eosinophilic inflammation as evident in studies of IL-4 Tg mice (38). Our studies of hORMDL3$^{zp3\text{-}Cre}$ mice confirmed that chemokines (CXCL10, CXCL11) we had observed to be highly expressed in vitro in ORMDL3-transfected cells (13) were highly expressed in hORMDL3$^{zp3\text{-}Cre}$ mice bronchial epithelium (CXCL10) and alveolar macrophages (CXCL11). Although asthma has predominantly been associated with expression of CC chemokines, CXC chemokines have also been linked to asthma in studies in humans with asthma (39–42), as well as in studies in animal models (43, 44) (i.e., CXCL10 knockout mice have significant reduction in Th2-type allergic airway inflammation and airway responsiveness) (43).

hORMDL3$^{zp3\text{-}Cre}$ mice also had increased levels of IgE without increases in IgG, IgM, or IgA. The level of OVA-specific IgE increased significantly more in hORMDL3$^{zp3\text{-}Cre}$ mice challenged with OVA compared to WT mice challenged with OVA. Because IL-4 and IL-13 switch B cells to IgE production (45), we examined whether either cytokine was increased in association with increases in OVA-specific IgE or increases in total IgE. The increase in OVA-specific IgE in hORMDL3$^{zp3\text{-}Cre}$ mice following acute OVA challenge was associated with increased levels of IL-4. In contrast, the increase in total IgE detected in hORMDL3$^{zp3\text{-}Cre}$ mice preceded the increase in IL-13. Preliminary studies did not demonstrate a difference in the number of splenic B cells expressing IgE in hORMDL3$^{zp3\text{-}Cre}$ compared to WT mice (data not shown). Further studies are needed to determine whether the increased total IgE and allergen-specific IgE production we have noted in hORMDL3$^{zp3\text{-}Cre}$ mice is due to either cytokines (IL-4, IL-13) or T cell and/or B cell pathways that are regulated by ORMDL3. In epidemiologic studies of asthma, chromosome 17q21 has been linked to IgE in some (5, 8) but not all studies (3, 7). Studies of ORMDL3 in Puerto Rican asthmatics have demonstrated a significant association between single nucleotide polymorphism (SNP) rs12603332 and $\log_{10}$ IgE levels (5), whereas subgroup analysis showed important associations between SNPs rs4378650 and rs12603332 in patients with allergic asthma (IgE $>$ 100 IU/ml). The association between these SNPs and asthma became stronger in patients with IgE levels $>$100 IU/ml (5).

In summary, these studies in hORMDL3$^{zp3\text{-}Cre}$ mice provide evidence that ORMDL3 plays an important role in activation of the ATF6 UPR pathway in vivo, and that expression of ORMDL3 in vivo regulates airway remodeling (smooth muscle, fibrosis, mucus) potentially through ATF6 target genes such as SERCA2b and/or through ATF6-independent genes (TGF-β1, ADAM8, MMP-9) detected in airway epithelium, as well as through as yet unidentified and/or uninvestigated pathways. In this regard sphingolipids are known to be regulated by ORMDL3, and sphingolipid pathways have been associated with asthma but not airway remodeling in mouse models (46–48). ORMDL3 also regulates ER-mediated calcium signaling (49) and lymphocyte activation in vitro (50). Because ORMDL3 is expressed in multiple cell types important to the pathogenesis of asthma (i.e., epithelial cells,

macrophages, eosinophils, T cells) (13, 51), in this study we have examined how increased expression of ORMDL3 in multiple cell types contributes to the pathogenesis of asthma. Future studies with selective overexpression of ORMDL3 in particular cell types will provide insight into the role of ORMDL3 in these individual cell types to the pathogenesis of asthma. Interestingly, increased levels of airway remodeling preceded increased levels of airway inflammation ($CD4^+$ cells, macrophages, eosinophils, neutrophils) in the lungs of $hORMDL3^{zp3\text{-}Cre}$ mice, suggesting that airway remodeling can be dissociated from these pathways by activation of ORMDL3. As airway remodeling can be detected not only in adults with asthma, but also in childhood asthma (52), increased expression of ORMDL3 in childhood asthmatics could contribute to the early development of airway remodeling. Overall, these studies provide preliminary evidence for an in vivo mechanism to link an ER-localized protein such as ORMDL3 to the pathogenesis of airway remodeling, airway hyperreactivity, and asthma.

Disclosures

The authors have no financial conflicts of interest.

References

1. Moffatt, M. F., M. Kabesch, L. Liang, A. L. Dixon, D. Strachan, S. Heath, M. Depner, A. von Berg, A. Bufe, E. Rietschel, et al. 2007. Genetic variants regulating ORMDL3 expression contribute to the risk of childhood asthma. *Nature* 448: 470–473.
2. Bouzigon, E., E. Corda, H. Aschard, M. H. Dizier, A. Boland, J. Bousquet, N. Chateigner, F. Gormand, J. Just, N. Le Moual, et al. 2008. Effect of 17q21 variants and smoking exposure in early-onset asthma. *N. Engl. J. Med.* 359: 1985–1994.
3. Moffatt, M. F., I. G. Gut, F. Demenais, D. P. Strachan, E. Bouzigon, S. Heath, E. von Mutius, M. Farrall, M. Lathrop, and W. O. Cookson; GABRIEL Consortium. 2010. A large-scale, consortium-based genomewide association study of asthma. *N. Engl. J. Med.* 363: 1211–1221.
4. Wan, Y. I., N. R. Shrine, M. Soler Artigas, L. V. Wain, J. D. Blakey, M. F. Moffatt, A. Bush, K. F. Chung, W. O. Cookson, D. P. Strachan, et al; Australian Asthma Genetics Consortium. 2012. Genome-wide association study to identify genetic determinants of severe asthma. *Thorax* 67: 762–768.
5. Galanter, J., S. Choudhry, C. Eng, S. Nazario, J. R. Rodríguez-Santana, J. Casal, A. Torres-Palacios, J. Salas, R. Chapela, H. G. Watson, et al. 2008. ORMDL3 gene is associated with asthma in three ethnically diverse populations. *Am. J. Respir. Crit. Care Med.* 177: 1194–1200.
6. Sleiman, P. M., K. Annaiah, M. Imielinski, J. P. Bradfield, C. E. Kim, E. C. Frackelton, J. T. Glessner, A. W. Eckert, F. G. Otieno, E. Santa, et al. 2008. ORMDL3 variants associated with asthma susceptibility in North Americans of European ancestry. *J. Allergy Clin. Immunol.* 122: 1225–1227.
7. Hirota, T., M. Harada, M. Sakashita, S. Doi, A. Miyatake, K. Fujita, T. Enomoto, M. Ebisawa, S. Yoshihara, E. Noguchi, et al. 2008. Genetic polymorphism regulating ORM1-like 3 (*Saccharomyces cerevisiae*) expression is associated with childhood atopic asthma in a Japanese population. *J. Allergy Clin. Immunol.* 121: 769–770.
8. Leung, T. F., H. Y. Sy, M. C. Ng, I. H. Chan, G. W. Wong, N. L. Tang, M. M. Waye, and C. W. Lam. 2009. Asthma and atopy are associated with chromosome 17q21 markers in Chinese children. *Allergy* 64: 621–628.
9. Binia, A., N. Khorasani, P. K. Bhavsar, I. Adcock, C. E. Brightling, K. F. Chung, W. O. Cookson, and M. F. Moffatt. 2011. Chromosome 17q21 SNP and severe asthma. *J. Hum. Genet.* 56: 97–98.
10. Marinho, S., A. Custovic, P. Marsden, J.A. Smith, and A Simpson. 2012. 17q12-21 variants are associated with asthma and interact with active smoking in an adult population from the United Kingdom. *Ann. Allergy Asthma Immunol.* 108: 402-411.e9.
11. Calışkan, M., Y. A. Bochkov, E. Kreiner-Møller, K. Bønnelykke, M. M. Stein, G. Du, H. Bisgaard, D. J. Jackson, J. E. Gern, R. F. Lemanske, Jr., et al. 2013. Rhinovirus wheezing illness and genetic risk of childhood-onset asthma. *N. Engl. J. Med.* 368: 1398–1407.
12. Hjemqvist, L., M. Tuson, G. Marfany, E. Herrero, S. Balcells, and R. Gonzalez-Durate. 2002. ORMDL proteins are a conserved new family of endoplasmic reticulum membrane proteins. *Genome Biol.* 3: RESEARCH0027.
13. Miller, M., A. B. Tam, J. Y. Cho, T. A. Doherty, A. Pham, N. Khorram, P. Rosenthal, J. L. Mueller, H. M. Hoffman, M. Suzukawa, et al. 2012. ORMDL3 is an inducible lung epithelial gene regulating metalloproteases, chemokines, OAS, and ATF6. *Proc. Natl. Acad. Sci. USA* 109: 16648–16653.
14. Walter, P., and D. Ron. 2011. The unfolded protein response: from stress pathway to homeostatic regulation. *Science* 334: 1081–1086.
15. Mahn, K., S. J. Hirst, S. Ying, M. R. Holt, P. Lavender, O. O. Ojo, L. Siew, D. E. Simcock, C. G. McVicker, V. Kanabar, et al. 2009. Diminished sarco/endoplasmic reticulum Ca^{2+} ATPase (SERCA) expression contributes to airway remodelling in bronchial asthma. *Proc. Natl. Acad. Sci. USA* 106: 10775–10780.
16. Cho, J. Y., M. Miller, K. J. Baek, J. W. Han, J. Nayar, S. Y. Lee, K. McElwain, S. McElwain, S. Friedman, and D. H. Broide. 2004. Inhibition of airway remodeling in IL-5-deficient mice. *J. Clin. Invest.* 113: 551–560.
17. Doherty, T. A., N. Khorram, K. Sugimoto, D. Sheppard, P. Rosenthal, J. Y. Cho, A. Pham, M. Miller, M. Croft, and D. H. Broide. 2012. Alternaria induces STAT6-dependent acute airway eosinophilia and epithelial FIZZ1 expression that promotes airway fibrosis and epithelial thickness. *J. Immunol.* 188: 2622–2629.
18. Prasad, K., and G. K. Prabhu. 2012. Image analysis tools for evaluation of microscopic views of immunohistochemically stained specimen in medical research: a review. *J. Med. Syst.* 36: 2621–2631.
19. Manzanero, S. 2012. Generation of mouse bone marrow-derived macrophages. *Methods Mol. Biol.* 844: 177–181.
20. Babour, A., A. A. Bicknell, J. Tourtellotte, and M. Niwa. 2010. A surveillance pathway monitors the fitness of the endoplasmic reticulum to control its inheritance. *Cell* 142: 256–269.
21. Brydges, S. D., J. L. Mueller, M. D. McGeough, C. A. Pena, A. Misaghi, C. Gandhi, C. D. Putnam, D. L. Boyle, G. S. Firestein, A. A. Horner, et al. 2009. Inflammasome-mediated disease animal models reveal roles for innate but not adaptive immunity. *Immunity* 30: 875–887.
22. Vignola, A. M., P. Chanez, G. Chiappara, A. Merendino, E. Pace, A. Rizzo, A. M. la Rocca, V. Bellia, G. Bonsignore, and J. Bousquet. 1997. Transforming growth factor-beta expression in mucosal biopsies in asthma and chronic bronchitis. *Am. J. Respir. Crit. Care Med.* 156: 591–599.
23. Redington, A. E., J. Madden, A. J. Frew, R. Djukanovic, W. R. Roche, S. T. Holgate, and P. H. Howarth. 1997. Transforming growth factor-β1 in asthma. Measurement in bronchoalveolar lavage fluid. *Am. J. Respir. Crit. Care Med.* 156: 642–647.
24. Wenzel, S. E., L. B. Schwartz, E. L. Langmack, J. L. Halliday, J. B. Trudeau, R. L. Gibbs, and H. W. Chu. 1999. Evidence that severe asthma can be divided pathologically into two inflammatory subtypes with distinct physiologic and clinical characteristics. *Am. J. Respir. Crit. Care Med.* 160: 1001–1008.
25. Lemjabbar, H., P. Gosset, C. Lamblin, I. Tillie, D. Hartmann, B. Wallaert, A. B. Tonnel, and C. Lafuma. 1999. Contribution of 92 kDa gelatinase/type IV collagenase in bronchial inflammation during status asthmaticus. *Am. J. Respir. Crit. Care Med.* 159: 1298–1307.
26. Hoshino, M., Y. Nakamura, J. Sim, J. Shimojo, and S. Isogai. 1998. Bronchial subepithelial fibrosis and expression of matrix metalloproteinase-9 in asthmatic airway inflammation. *J. Allergy Clin. Immunol.* 102: 783–788.
27. Foley, S. C., A. K. Mogas, R. Olivenstein, P. O. Fiset, J. Chakir, J. Bourbeau, P. Ernst, C. Lemière, J. G. Martin, and Q. Hamid. 2007. Increased expression of ADAM33 and ADAM8 with disease progression in asthma. *J. Allergy Clin. Immunol.* 119: 863–871.
28. Phipps, S., F. Benyahia, T. T. Ou, J. Barkans, D. S. Robinson, and A. B. Kay. 2004. Acute allergen-induced airway remodeling in atopic asthma. *Am. J. Respir. Cell Mol. Biol.* 31: 626–632.
29. Kariyawasam, H. H., S. Pegorier, J. Barkans, G. Xanthou, M. Aizen, S. Ying, A. B. Kay, C. M. Lloyd, and D. S. Robinson. 2009. Activin and transforming growth factor-β signaling pathways are activated after allergen challenge in mild asthma. *J. Allergy Clin. Immunol.* 124: 454–462.
30. Kelly, E. A., W. W. Busse, and N. N. Jarjour. 2000. Increased matrix metalloproteinase-9 in the airway after allergen challenge. *Am. J. Respir. Crit. Care Med.* 162: 1157–1161.
31. Cataldo, D. D., K. G. Tournoy, K. Vermaelen, C. Munaut, J. M. Foidart, R. Louis, A. Noël, and R. A. Pauwels. 2002. Matrix metalloproteinase-9 deficiency impairs cellular infiltration and bronchial hyperresponsiveness during allergen-induced airway inflammation. *Am. J. Pathol.* 161: 491–498.
32. Lim, D. H., J. Y. Cho, M. Miller, K. McElwain, S. McElwain, and D. H. Broide. 2006. Reduced peribronchial fibrosis in allergen-challenged MMP-9-deficient mice. *Am. J. Physiol. Lung Cell. Mol. Physiol.* 291: L265–L271.
33. King, N. E., N. Zimmermann, S. M. Pope, P. C. Fulkerson, N. M. Nikolaidis, A. Mishra, D. P. Witte, and M. E. Rothenberg. 2004. Expression and regulation of a disintegrin and metalloproteinase (ADAM) 8 in experimental asthma. *Am. J. Respir. Cell Mol. Biol.* 31: 257–265.
34. Naus, S., M. R. Blanchet, K. Gossens, C. Zaph, J. W. Bartsch, K. M. McNagny, and H. J. Ziltener. 2010. The metalloprotease-disintegrin ADAM8 is essential for the development of experimental asthma. *Am. J. Respir. Crit. Care Med.* 181: 1318–1328.
35. Le, A. V., J. Y. Cho, M. Miller, S. McElwain, K. Golgotiu, and D. H. Broide. 2007. Inhibition of allergen-induced airway remodeling in Smad 3-deficient mice. *J. Immunol.* 178: 7310–7316.
36. McMillan, S. J., G. Xanthou, and C. M. Lloyd. 2005. Manipulation of allergen-induced airway remodeling by treatment with anti-TGF-β antibody: effect on the Smad signaling pathway. *J. Immunol.* 174: 5774–5780.
37. Adachi, Y., K. Yamamoto, T. Okada, H. Yoshida, A. Harada, and K. Mori. 2008. ATF6 is a transcription factor specializing in the regulation of quality control proteins in the endoplasmic reticulum. *Cell Struct. Funct.* 33: 75–89.
38. Rankin, J. A., D. E. Picarella, G. P. Geba, U. A. Temann, B. Prasad, B. DiCosmo, A. Tarallo, B. Stripp, J. Whitsett, and R. A. Flavell. 1996. Phenotypic and physiologic characterization of transgenic mice expressing interleukin 4 in the lung: lymphocytic and eosinophilic inflammation without airway hyperreactivity. *Proc. Natl. Acad. Sci. USA* 93: 7821–7825.
39. Norzila, M. Z., K. Fakes, R. L. Henry, J. Simpson, and P. G. Gibson. 2000. Interleukin-8 secretion and neutrophil recruitment accompanies induced sputum eosinophil activation in children with acute asthma. *Am. J. Respir. Crit. Care Med.* 161: 769–774.

40. Jatakanon, A., C. Uasuf, W. Maziak, S. Lim, K. F. Chung, and P. J. Barnes. 1999. Neutrophilic inflammation in severe persistent asthma. *Am. J. Respir. Crit. Care Med.* 160: 1532–1539.
41. Ying, S., B. O'Connor, J. Ratoff, Q. Meng, C. Fang, D. Cousins, G. Zhang, S. Gu, Z. Gao, B. Shamji, et al. 2008. Expression and cellular provenance of thymic stromal lymphopoietin and chemokines in patients with severe asthma and chronic obstructive pulmonary disease. *J. Immunol*. 181: 2790–2798.
42. Bochner, B. S., S. A. Hudson, H. Q. Xiao, and M. C. Liu. 2003. Release of both CCR4-active and CXCR3-active chemokines during human allergic pulmonary late-phase reactions. *J. Allergy Clin. Immunol.* 112: 930–934.
43. Medoff, B. D., A. Sauty, A. M. Tager, J. A. Maclean, R. N. Smith, A. Mathew, J. H. Dufour, and A. D. Luster. 2002. IFN-γ-inducible protein 10 (CXCL10) contributes to airway hyperreactivity and airway inflammation in a mouse model of asthma. *J. Immunol.* 168: 5278–5286.
44. Lin, Y., H. Yan, Y. Xiao, H. Piao, R. Xiang, L. Jiang, H. Chen, K. Huang, Z. Guo, W. Zhou, et al. 2011. Attenuation of antigen-induced airway hyperresponsiveness and inflammation in CXCR3 knockout mice. *Respir. Res.* 12: 123.
45. Burton, O. T., and H. C. Oettgen. 2011. Beyond immediate hypersensitivity: evolving roles for IgE antibodies in immune homeostasis and allergic diseases. *Immunol. Rev.* 242: 128–143.
46. Breslow, D. K., S. R. Collins, B. Bodenmiller, R. Aebersold, K. Simons, A. Shevchenko, C. S. Ejsing, and J. S. Weissman. 2010. Orm family proteins mediate sphingolipid homeostasis. *Nature* 463: 1048–1053.
47. Worgall, T.S., A. Veerappan, B. Sung, B.I. Kim, E. Weiner, R. Bholah, R.B. Silver, X.C. Jiang, and S. Worgall. 2013. Impaired sphingolipid synthesis in the respiratory tract induces airway hyperreactivity. *Sci. Transl. Med.* 5: 186ra67.
48. Levy, B. D. 2013. Sphingolipids and susceptibility to asthma. *N. Engl. J. Med.* 369: 976–978.
49. Cantero-Recasens, G., C. Fandos, F. Rubio-Moscardo, M. A. Valverde, and R. Vicente. 2010. The asthma-associated ORMDL3 gene product regulates endoplasmic reticulum-mediated calcium signaling and cellular stress. *Hum. Mol. Genet.* 19: 111–121.
50. Carreras-Sureda, A., G. Cantero-Recasens, F. Rubio-Moscardo, K. Kiefer, C. Peinelt, B. A. Niemeyer, M. A. Valverde, and R. Vicente. 2013. ORMDL3 modulates store-operated calcium entry and lymphocyte activation. *Hum. Mol. Genet.* 22: 519–530.
51. Ha, S. G., X. N. Ge, N. S. Bahaie, B. N. Kang, A. Rao, S. P. Rao, and P. Sriramarao. 2013. ORMDL3 promotes eosinophil trafficking and activation via regulation of integrins and CD48. *Nat Commun.* 4: 2479.
52. Malmström, K., A. S. Pelkonen, and M. J. Mäkelä. 2013. Remodeling, inflammation and airway responsiveness in early childhood asthma. *Curr. Opin. Allergy Clin. Immunol.* 13: 203–210.